ΔV Optimized Interplanetary Trajectories to Uranus

Gene Luevano

Table of Contents

ΔV Optimized Interplanetary Trajectories to Uranus

Gene Luevano

To minimize the Delta-V required to send spacecraft to Uranus, a trajectory with multiple gravity assists must be used. However, the process of finding the optimal trajectory is too complicated to be found by hand. To make this task more feasible, this project employed the use of genetic algorithms to effectively explore the solution space to identify viable trajectories. To verify and validate the results of the genetic algorithm, NASA's Galileo mission to Jupiter was recreated. The algorithm produced a mission profile that was accurate within ± 8.2% of Galileo's real flight data, including the key dates, required injection energy, and total Delta-V. After verifying and validating the capabilities of the genetic algorithm, the genetic algorithm was then set up to study possible interplanetary trajectories to Uranus. After 12 hours of parallel computation, the genetic algorithm was able to produce 60 unique trajectories between Earth and Uranus.

Nomenclature

ΔV	=	change in velocity
T_0	=	departure date
N	=	number of gravity assists
P	=	planet number
T	=	duration between gravity assists
$\vec{v}_\infty$	=	in/out relative velocity
$\vec{V}_S$	=	spacecraft heliocentric velocity
$\vec{V}_P$	=	planet velocity
a	=	orbit semi-major axis
μ_P	=	planet mass parameter
δ	=	hyperbolic turning angle
e	=	orbit eccentricity
r_p	=	gravity assist periapsis
V_d	=	planetary departure velocity
C3	=	orbit injection energy
V_p	=	periapsis velocity
E	=	orbital energy
r_{SOI}	=	sphere of influence radius
k	=	minimum flyby radius parameter
R_P	=	mean planetary radius
N_P	=	number of planet orbits
N_{SC}	=	number of spacecraft orbits

1. Introduction

The ice giant Uranus is one of the most unique planets in the solar system. Orbiting at an average distance of 20 astronautical units (AU), 1 AU being the average distance between the Earth and the Sun, this blue-green planet is tilted over 90° from the plane of its orbit. The current theory at the National Aeronautics and Space Administration (NASA) suggests that Uranus's tilt was possibly "the result of a collision with an Earth-size object long ago" [1]. Unfortunately, there have not been any dedicated science missions by any organization on Earth to the outer planet. However, the planet has not gone unvisited. Almost 40 years ago in January of 1986, Voyager 2 made a fly-by of the planet during its grand tour of the outer solar system. While in Uranus' sphere of influence, Voyager 2 discovered 10 new moons and 2 additional rings around the planet [2].

Yet, in the past 40 years, there have been no follow-up missions to Uranus. This has likely been due to a lack of funding or other higher scientific priorities, such as studying Jupiter and Saturn. At the time of writing this paper, there have been four missions to Jupiter;

Galileo, Juno, the Jupiter Icy Moons Explorer (JUICE), and Europa Clipper, and one mission to Saturn, Cassini. While Galileo and Cassini have long since retired, Juno is in the final stages of its operational life [3], The European Space Agency's (ESA) JUICE mission is one year into its 8-year trajectory to Jupiter [4], and the Europa Clipper mission is planned to launch in October of 2024 [5]. However, after JUICE and the Europa Clipper are expected to conclude their missions in the mid-2030s, there have not been any announced plans for science missions to the outer planets.

Identifying this gap, the National Academies of Sciences, Engineering, and Medicine provided NASA with a recommendation for its next flagship mission, a Uranus orbiter and probe. The mission "will deliver an in situ atmospheric probe and conduct a multi-year orbital tour that will transform our knowledge of ice giants in general and the uranian system in particular" [6]. The corresponding scientific objectives for this mission are expected to address Uranus's "(1) origin, interior, and atmosphere; (2) magnetosphere; and (3) satellites and rings" [6]. While these objectives are being finalized over the next several years, the viable launch windows have already been identified. The most optimal trajectories would require a departure sometime between 2031 and 2032. During this time frame, Jupiter is in an ideal position to be used as a gravity assist to kick the spacecraft out to Uranus. From 2033-2038, other trajectory options are available but they require the use of inner solar system gravity assists and as a result have greater trajectory flight time [6, 7].

While the interplanetary trajectories identified by the John Hopkins Applied Physics Laboratory [7] needed to consider the spacecraft mass budget, time of flight, total flight ΔV, and the satellite tour upon arrival to Uranus, the goal of this project is to identify ΔV optimized interplanetary trajectories using gravity assists from Earth to Uranus. In the following sections, a breakdown will be provided of the project methodology, validation and verification, results, conclusions drawn, future work, and the lessons learned during the development of the project.

2. Project Methodology

One of the easiest ways to lower the total required spacecraft ΔV is to use multiple gravity assists. According to NASA, "[the] "gravity assist" flyby technique can add or subtract momentum to increase or decrease the energy of a spacecraft's orbit" [8]. This maneuver-free momentum change is possible due to the change in the gravitational forces felt by the spacecraft. During each fly-by, the spacecraft's inbound velocity is rotated and the closer it becomes aligned with the planet's velocity vector about the sun, the greater the momentum imparted on the spacecraft. Sometimes, additional orbital energy is required and either the fly-by altitude can be lowered or an impulse maneuver can be performed to get the desired velocity after the gravity assist. Additionally, trajectories that perform a deep space maneuver can also reduce the total ΔV requirements of a spacecraft. However, these maneuvers will not be considered in the trajectories for this project.

Between Mercury and Saturn, there are hundreds, if not thousands, of ways to chain together gravity assists from Earth to Uranus. Also accounting for departure dates and the time between gravity assists, there are too many permutations of mission parameters to be computed. Instead of using brute force, an optimization algorithm should be employed to quickly and effectively determine ΔV minimized solutions. For this project, a genetic algorithm was employed to quickly explore the solution space for possible trajectories as well as minimize the ΔV requirement of those solutions with multiple runs of the algorithm.

2.1 Genetic Algorithm Description

The genetic algorithm (GA) is an approach to cost function optimization that treats the variables to be optimized as genes, the array of variables as chromosomes, and the collection of arrays as the population. Provided an upper and lower bound, the genes within the initial chromosomes are randomized and provided a score based on the user-provided cost function. The algorithm will select the chromosomes that received the lowest cost value and will perform a

pseudo-evolution to create the next generation of genes that will try to improve on the lowest overall cost [9-11]. This process is repeated for several hundred iterations, evolving and improving the genes that are used to produce the smallest cost. Once the smallest cost value has not improved after several generations, or the entire population converges to what it calculates to be the best cost for the evolved chromosomes, the algorithm will stop and return the chromosome with the genes that best minimize its cost function. However, due to the random nature of the initial value assignments and the use of a non-linear cost function, there is no way to know for certain that the best chromosome set is the best solution, but one of many possible local minimums. To minimize that concern for this project, once a viable trajectory was identified its number of gravity assists and corresponding order were fixed. Fixing these values allowed the GA to focus on optimizing the times of flight between each gravity assist the best it could. Each trajectory was rerun 5 times to increase the number of opportunities for a more effective trajectory to be identified over what was originally found.

2.2 Interplanetary Mission Design Using Genetic Algorithms

Before using the GA to solve for interplanetary trajectories, first the key assumptions for the project must be made. The following assumptions help simplify the possible solutions to the complex problem of interplanetary trajectory design.

1. The Uranus-bound spacecraft will use an inertial upper stage (IUS) to supplement the required orbital injection energy from its parking orbit around Earth.
2. The interplanetary trajectory will use multiple gravity assists.
3. The spacecraft will perform impulse maneuvers only at the close approaches of each gravity assist if necessary.
4. Each trajectory will be modeled using the patched-conic method and propagated using the two-body dynamics problem.

In conjunction with the aforementioned assumptions, the solutions to Lambert's problem will be used as the arrival and departure velocities during each gravity assist [12, 13]. To get the state of the gravity assists planets for use in Lambert's problem, NASA's Navigation and Ancillary Information Facility (NAIF) offers researchers access to the tool SPICE (Spacecraft, Planet, Instrument, C-matrix, Events). SPICE is an "observation geometry information system to assist scientists in planning and interpreting scientific observations from space-based instruments aboard robotic planetary spacecraft" [14-16]. However, the SPICE tool needs additional information from NAIF's Planetary Data System (PDS) to support the work of this project. In particular, the SPICE tool needs access to the latest planetary ephemerides [17, 18] and leap seconds information [19, 20] to provide accurate planet state information that in turn will help produce accurate trajectory solutions to Lambert's problem.

Using the established assumptions, the decision variables that are needed by the GA to optimize the required ΔV can be identified. The expected decision variables for the GA are the departure date, number of gravity assists, and the order of the gravity assists. However, there are additional decision variables that also need to be considered. To get the solutions to Lambert's problem the initial planet's position, the terminal planet's position, and the time of flight between the two states must be known. If the solutions to Lambert's problem are being used to predict the gravity assists, then the states of the planets are simply functions of time since the original departure date. These times can then be broken down into the length of time between gravity assists and are the remaining decision variables for the GA [21, 22]. An example of a chromosome containing all of the decision variables can be seen below.

$$\mathbf{X} = [T_0, N, P_1, \ldots, P_N, T_1, \ldots, T_N, T_f] \quad (1)$$

However, since one of the decision variables is the number of gravity assists to be performed, it shapes how many variables are to be considered. Unfortunately, when using MATLAB's function "ga" it does not take into account the dynamic number of variables to be optimized [23]. So, to prevent errors being thrown in the code, a chromosome large enough to contain the information for a trajectory using the user-defined maximum number of gravity assists must be provided to the GA. Although there will be some chromosomes that are using less than the maximum number of gravity assists, the extra variables are not used to affect the cost function and thus are treated as "hidden genes" [22, 24].

Now, with the variables to be optimized by the GA identified, the next step is to define the cost function the decision variables will be used to score. For this project, the cost function, C, is the addition of f(**X**), the sum of the required ΔVs, with the penalties incurred for poor trajectories selected by the GA, g(**X**).

$$C = f(\mathbf{X}) + g(\mathbf{X}) \tag{2}$$

2.2.1 Cost Function ΔVs

To determine the required ΔV for each interplanetary trajectory, the following approach was followed [21, 22]. For each gravity assist within the trajectory, the relative inbound and outbound velocities are found by taking the difference between the solutions to Lambert's problem and the velocity of the planet during the gravity assist.

$$\vec{v}_{\infty,\,in} = \vec{V}_{S,\,in} - \vec{V}_P \tag{3}$$

$$\vec{v}_{\infty,\,out} = \vec{V}_{S,\,out} - \vec{V}_P \tag{4}$$

If the magnitudes of the inbound and outbound relative velocities are equal, then the gravity assist is deemed "unpowered". In this case, there is no impulse performed at the periapsis of the gravity assist and the trajectory within the sphere of influence is continuous. However, if the magnitudes of the inbound and outbound velocities are not equal, then a powered flyby must be performed and a discontinuity is created in the flyby. Should this be the case, the periapsis radius where the inbound and outbound trajectories meet must be found. To determine this value, the first step is to calculate the inbound and outbound hyperbolic semi-major axes.

$$a_{in} = \frac{-\mu_P}{||\vec{v}_{\infty,\,in}||} \tag{5}$$

$$a_{out} = \frac{-\mu_P}{||\vec{v}_{\infty,\,out}||} \tag{6}$$

The second step is to calculate the turning angle between the inbound and outbound velocities.

$$\delta = \cos^{-1}\left(\frac{\vec{v}_{\infty,\,in} \bullet \vec{v}_{\infty,\,out}}{||\vec{v}_{\infty,\,in}||\,||\vec{v}_{\infty,\,out}||}\right) \tag{7}$$

The turning angle of the gravity assist can also be rewritten to be solved as a function of the inbound and outbound eccentricities.

$$\delta = \sin^{-1}\left(\frac{1}{e_{in}}\right) + \sin^{-1}\left(\frac{1}{e_{out}}\right) \tag{8}$$

For Eq. (8) to be valid, the following equations for the periapsis radius must be true because, with this approach, the periapsis radius must be equal for both legs of the flyby.

$$r_p = a_{in}(1 - e_{in}) = a_{out}(1 - e_{out}) \tag{9}$$

Unfortunately, the variables e_{in} and e_{out} are unknown so Eqs. (8) and (9) are not easily solvable. However, if Eqs. (8) and (9) are rearranged into a single equation that is a function of one unknown, e_{out}, it can be used in an iterative root finder, such as the Newton-Raphson method, to find the outbound eccentricity.

$$f(e_{out}) = \left(\left(\frac{a_{out}}{a_{in}}\right)(e_{out} - 1)\right) * \sin\left(\delta - \sin^{-1}\left(\frac{1}{e_{out}}\right)\right) - 1 = 0 \quad (10)$$

Additionally, to use the Newton-Raphson method, the first derivative of Eq. (10) with respect to e_{out} must be known.

$$\frac{df(e_{out})}{de_{out}} = \left(\frac{a_{out}}{a_{in}} e_{out} - \frac{a_{out}}{a_{in}} + 1\right) * \frac{cos(\delta - sin^{-1}(\frac{1}{e_{out}}))}{e_{out}^2\sqrt{1-\frac{1}{e_{out}^2}}} + \frac{a_{out}}{a_{in}}\sin\left(\delta - \sin^{-1}\left(\frac{1}{e_{out}}\right)\right) \quad (11)$$

Using Eqs. (10) and (11), the equation to find the new value of e_{out} based on a previously estimated value for e_{out} can be written as below.

$$e_{new} = e_{old} - \frac{f(e_{old})}{\frac{df(e_{old})}{de_{out}}} \quad (12)$$

For this project, the initial value for e_{out} used was 1.5 and the method was allowed up to 200 loop iterations to converge. If the value for e_{out} did not converge, then MATLAB's "fsolve" function was used to find the outbound eccentricity [25]. With the value for e_{out} now known, the next step is to calculate r_p using Eq. (9) which patches the inbound and outbound trajectories together. Finally, with r_p, the ΔV required at the periapsis of the gravity assist to move from the inbound trajectory to the outbound trajectory can be calculated using the following equation.

$$\Delta V_{flyby} = \left|\sqrt{||\vec{v}_{\infty, in}||^2 + \frac{2\mu_P}{r_p}} - \sqrt{||\vec{v}_{\infty, out}||^2 + \frac{2\mu_P}{r_p}}\right| \quad (13)$$

In addition to the ΔVs required during each gravity assist, the ΔVs to leave low Earth orbit and be captured about Uranus must also be calculated. The two equations needed for these calculations are very similar to Eq. (13). For the departure trajectory from Earth, provided the injection energy of the assumed IUS is known, the calculation for the required ΔV will only be necessary if the required Earth outbound velocity is more than what can be provided by the IUS.

$$V_{d, potential} = \sqrt{C3 + \frac{2\mu_P}{r_{parking}}} \quad (14)$$

$$V_{d, required} = \sqrt{||\vec{v}_{\infty, out}||^2 + \frac{2\mu_P}{r_{parking}}} \quad (15)$$

$$\Delta V_{depart} = \begin{cases} V_{d, required} - V_{d, potential} ; V_{d, potential} < V_{d, required} \\ 0 ; V_{d, potential} \geq V_{d, required} \end{cases} \quad (16)$$

To determine the required ΔV for the Uranus orbit insertion, the parameters of the capture orbit must be known. For this project, it is assumed that the target orbit has a periapsis radius of 300,000 km and an eccentricity of 0.998. With these values, it can then be determined how much slower the spacecraft will need to be moving to be captured by Uranus.

$$a_{capture} = \frac{r_{p, capture}}{1 - e_{capture}} \quad (17)$$

$$V_{p, capture} = \sqrt{\frac{(1+e_{capture})\mu_P}{(1-e_{capture})a_{capture}}} \quad (18)$$

$$\Delta V_{capture} = \sqrt{||\vec{v}_{\infty, in}||^2 + \frac{2\mu_P}{r_{p, capture}}} - V_{p, capture} \quad (19)$$

After calculating the required ΔVs, they can be summed together to get the ΔV contribution to the cost function.

$$f(\mathbf{X}) = \Delta V_{depart} + \Delta V_{capture} + \sum_{i=1}^{N} \Delta V_{flyby, i} \quad (20)$$

2.2.2 Cost Function Penalties

With the random assignment of values from the GA, there is a chance that there will be poor trajectories as a result. A poor trajectory during a gravity assist will enter the planet's sphere of influence with not enough orbital energy to be hyperbolic, effectively captured in orbit about the planet, and or its flyby radius will be too low, entering the atmosphere or crashing into the surface. With these constraints in mind, a penalty needs to be applied to these trajectories to prevent them from being considered optimal trajectory options by the GA [21, 22, 26]. The orbital energy of an orbit can be calculated using the equation below.

$$E = \frac{||\vec{v}_{\infty, in}||^2}{2} - \frac{\mu_P}{r_{SOI}} \quad (21)$$

For an orbit to be hyperbolic, the value of E must be a positive number greater than or equal to 0. "However, the sphere of influence model is an approximation, so an additional 10% margin on the incoming velocity needs to be added" [22]. So, Eq. (21) can be rewritten to account for the additional 10%.

$$E = \frac{||0.9\vec{v}_{\infty, in}||^2}{2} - \frac{\mu_P}{r_{SOI}} \quad (22)$$

Should the energy of the trajectory be less than 0, its penalty contribution to the cost function will be the inverse of the magnitude of the inbound relative velocity. If the corresponding velocity to the low-energy orbit is high, then the contribution will be near zero. However, if the inbound trajectory has low energy and low velocity then its penalty contribution will be large. This significant penalty will shape the final solution away from parameters that lead to the poor trajectory.

$$g_{energy, i}(\mathbf{X}) = \begin{cases} 0 & ; E \geq 0 \\ \frac{1}{||\vec{v}_{\infty, in, i}||} & ; E < 0 \end{cases} \quad (23)$$

On the other hand, the other penalty constraint on the GA is for low altitude passes during the gravity assist. The threshold to determine what is the minimum acceptable gravity assist radius is user-defined, the factor *k* times the planet's radius. If the value of r_p from Eq. (9) is less than the minimum acceptable value, then this penalty is applied to shape the final solution away from the poor trajectory. Otherwise, the constraint is not violated and no penalty will be applied to the cost function.

$$g_{altitude, i}(\mathbf{X}) = \begin{cases} 0 & ; r_{p, i} \geq kR_{P, i} \\ -10log(\frac{r_{p, i}}{kR_{P, i}}) & ; r_{p, i} < kR_{P, i} \end{cases} \quad (24)$$

In addition to summing up the total amount of ΔV required, the next step is to sum up the penalties for each of the gravity assists.

$$g(\mathbf{X}) = \sum_{i=1}^{N} (g_{energy, i}(\mathbf{X}) + g_{altitude, i}(\mathbf{X})) \quad (25)$$

2.2.3 Consideration for Resonant Orbits

When performing multiple gravity assists, it becomes possible for a resonance orbit between two passes of the same planet to occur. A perfect resonance orbit will return a spacecraft to its initial position after 1 or more complete revolutions. However, the traditional approach to getting solutions for Lambert's problem cannot determine valid trajectories where the original position is exactly, or very close to, the terminal position for long times of flight. For a leg of the interplanetary trajectory to be identified as resonant for this project, its

travel time between gravity assists of the same planet had to be within ± 2 days of 1 or more complete revolutions of the respective planet [22]. However, there was a typo in Eq. (34) of [22], the integer number of orbits for the spacecraft and the planet were inverted, and it has been corrected in the following equation.

$$\left| T_i - \frac{N_P}{N_{SC}} T_{P,i} \right| \leq 2 \text{ days} \quad (26)$$

To account for possible resonance orbits and still be able to use a Lambert's problem solver, the method used was developed by R. H. Gooding [13] and its corresponding code was written by D. Eagle [27]. In this approach, Gooding devised a way to account for the number of complete revolutions between the initial and final states and successfully calculate a viable trajectory. Then, to determine if any ΔV was required to enter the resonance orbit, Eq. (13) was used based on the results of Gooding's solutions to Lambert's problem. Although the resonance orbit is supposed to use an unpowered flyby, this method shapes the final result of the GA to include a preliminary transfer that has enough energy to place the spacecraft into a resonance orbit. During testing, some interplanetary trajectories had legs from the prior gravity assists that did not approach the first pass of the resonance orbit with enough energy to match the requirements of the outbound trajectory. The assumption was that no correction to the inbound velocity was needed so the ΔV requirement for the first gravity assist was always set equal to 0 km/sec. However, further analysis of some trajectories showed that this assumption was flawed and the ΔV requirement for the gravity assist needed to be considered. Now, if a resonance orbit is possible, the GA will optimize the interplanetary trajectory such that the resonant orbit injection will require a near 0 km/sec impulse. This will be evident in Section 3 during the recreation of NASA's Galileo mission trajectory.

3. Project Verification and Validation

To verify and validate that the approach laid out in Section 2 is valid, it must be tested to see if it recreates an existing interplanetary mission that uses multiple gravity assists. In particular, the GA is expected to generate a trajectory with similar dates of departure, close approach, and arrival; amounts of injection energy; total required ΔV to perform the trajectory; and flyby altitudes during each gravity assist. Should a comparable trajectory be produced by the GA, it can be asserted that the GA can also find a valid trajectory from Earth to Uranus using the appropriate upper and lower bounds for the decision variables.

For this project, the GA was tasked to recreate NASA's mission to Jupiter, Galileo. The Galileo mission began in October 1989 after deploying from the Space Shuttle Atlantis. Leaving low Earth orbit Galileo used an IUS, with an injection energy of 17 km^2/s^2, to launch itself onto an intercept trajectory with Venus. The gravity assist from Venus placed the spacecraft on track to intercept Earth about 10 months later, after which the spacecraft would enter a resonance orbit and perform a second flyby of Earth two years later. After the second Earth flyby, the spacecraft finally had enough energy to reach the orbit of Jupiter. The final leg of the interplanetary trajectory was just shy of 3 years, leading to a total time of flight of 6 years. To maintain this trajectory, Galileo was required to perform about 200 m/sec of ΔV for trajectory corrections. Upon arrival at Jupiter, Galileo had to expend an additional 630 m/sec for its Jupiter insertion orbit maneuver to place itself into an orbit with an eccentricity of 0.998 and a periapsis radius of 286,000 km [28, 29].

During the initial tests for verification and validation, the recreation of Galileo's trajectory followed the routine detailed in Section 4.A in [22]. While Galileo's exact route was identified by the GA used in this project, its corresponding dates and ΔVs did not closely resemble Galileo's journey. This was likely due to the many possible permutations by such a large range in the upper and lower bounds. To increase the likelihood of the GA recreating Galileo's trajectory, the bounds of the decision

variables were constrained. The GA was given a 2-month window around Galileo's real departure date to find the optimal trajectory using 3 flybys, 1 of Venus and 2 of Earth. Additionally, the times of flight for each leg of the trajectory were constrained to be within ±10 days of the real mission values. The range for the final leg of the mission was ±20 days from the real flight data because, with the range of ±10 days, a good solution would not occur. Through several iterations of testing, it was identified that a range of ±20 days for the last leg of the trajectory was a quality constraint.

Table 3.1 - Decision Variable Constraints for the Genetic Algorithm

	T_0	N	P_1	P_2	P_3	T_1	T_2	T_3	T_f
Lower Bound	Oct 1, 1989	3	Venus	Earth	Earth	105	291	721	1064
Upper Bound	Nov 30, 1989	3	Venus	Earth	Earth	125	311	741	1124

Once the GA was provided with the constraints listed in the table above, it was able to converge onto a good solution that closely replicated the mission profile of Galileo. Although there are some slight differences between the trajectory created by the GA and the Galileo Flight Data, there is still a close resemblance to real-world data. Looking through Table 3.2, it can be seen that the dates as a part of the result of the GA are within 3-33 days of the real flight data [28]. Throughout the entire mission, this difference accounts for 0.15% to 1.5% of the total time of flight and would be within an acceptable margin of error. Moving to the next pair of columns, the orbital injection energy, it can be seen that the amount of injection energy required by Galileo and its GA recreation are both less than what was capable by the IUS. Although the GA's solution requires an additional 1 km^2/sec^2, it is only 8.2% larger than Galileo's required injection energy.

While the GA designed for this project only looks to optimize the planet-to-planet gravity assists, Galileo performed deep space maneuvers to encounter two asteroids, Gaspra and Ida. While Gaspra was visited during the resonant orbit between passes of Earth, the maneuvers to intercept Ida would have altered the trajectory produced by the gravity assist from Venus. By deviating from the original trajectory, it can be explained why Galileo not only had a higher ΔV requirement but also why it arrived 1 month before the GA solution. Another reason why Galileo had to expend more ΔV the GA solution may be because of the N-body problem gravitational perturbations. As Galileo got closer to Jupiter, its orbit was increasingly affected by Jupiter's gravity. As described in the assumptions of Section 2, the dynamics model used for this project was the two-body problem and thus it cannot account for the external gravitational perturbations. Finally, in the last column, the flyby altitudes for each gravity assist can be compared. Although this series of data may not appear to contribute much information, it does provide a mental picture of the turning angles for each flyby. When rearranging Eqs. (8) and (9), it can be seen that for a given inbound and outbound semi-major axis the turning angle can be written as a function of the periapsis radius.

$$\delta = \sin^{-1}\left(\frac{a_{in}}{a_{in}-r_p}\right) + \sin^{-1}\left(\frac{a_{out}}{a_{out}-r_p}\right) \quad (26)$$

As seen in Table 3.2, the altitude of the closest approach during the first gravity assist from Earth, as calculated by the GA, was greater than the real mission data. The flyby radius was 1.6 times greater than Galileo's trajectory, and as a result, led to a smaller turning angle during the gravity assist. Looking at Fig. 1, the effect of

Table 3.2 - Comparison of Galileo Flight Data to the Results of the Genetic Algorithm

	Date (Galileo)	Date (GA)	C3 (km^2/sec^2, Galileo)	C3 (km^2/sec^2, GA)	ΔV (km/sec, Galileo)	ΔV (km/sec, GA)	Altitude (km, Galileo)	Altitude (km, GA)
Earth Departure	Oct 18, 1989	Oct 28, 1989	13.5	14.6	-	-	296	296
Venus Close Approach (1)	Feb 10, 1990	Feb 13, 1990	-	-	-	$2.6x10^{-5}$	16,123	23,940
Earth Close Approach (1)	Dec 8, 1990	Dec 11, 1990	-	-	-	$3.6x10^{-4}$	960	5,671
Earth Close Approach (2)	Dec 8, 1992	Dec 11, 1992	-	-	-	0.0314	303	2,819
Jupiter Arrival	Dec 7, 1995	Jan 9, 1996	-	-	0.630	0.559	286,000	286,000

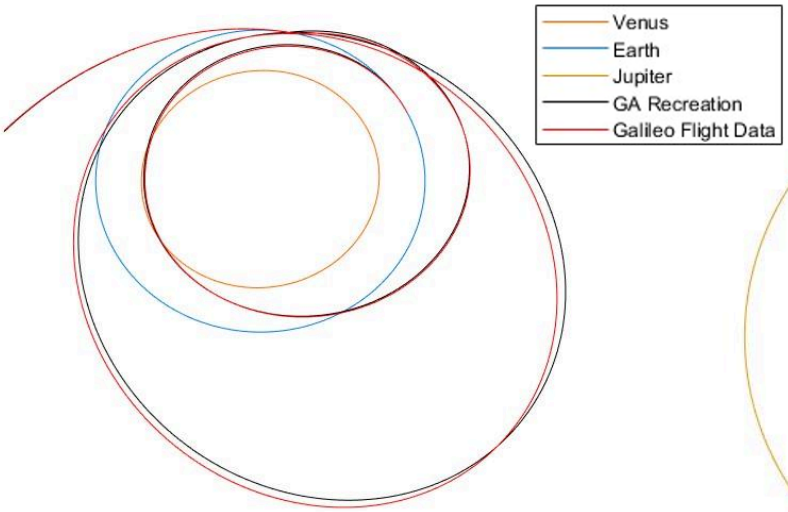

Fig. 1. Inner Solar System Trajectories

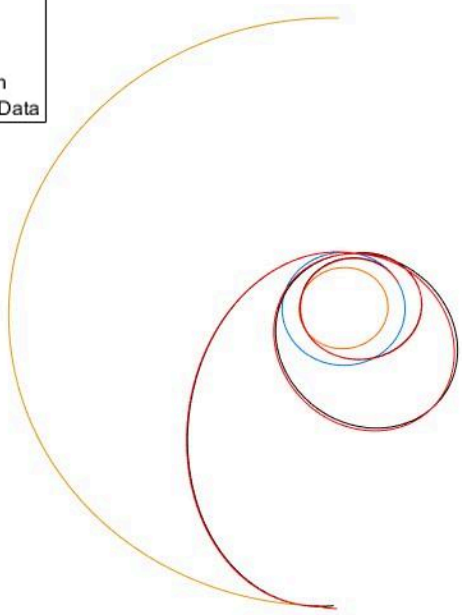

Fig. 2. Complete Solar System Trajectories

the lesser turning angle can be seen between the two Earth gravity assists. Of the 4 legs of the interplanetary trajectory, the leg between the two Earth gravity assists was the least accurate as the orbit tracks did not closely align. However, the remaining 3 legs all closely resemble the flight data for Galileo.

Another way to verify the work of the GA is to compare the two-body propagation of its optimized trajectory with the flight data of Galileo from NASA [30, 31]. However, because the two trajectories have different departure dates, the comparison metric will be the magnitude of their

positions from launch, day 0, to their captures at Jupiter.

Looking at Fig. 3, it can be seen that the two trajectories align very closely. At the end of the Galileo trajectory, however, it can be seen that there is a slight difference between the two trajectories. This difference comes from the fact that the Galileo mission enters its orbit around Jupiter one month before the GA recreation arrives at its periapsis to perform the Jupiter insertion orbit. To better analyze the data from Fig. 3, the differences in position magnitude between the two routes should be studied.

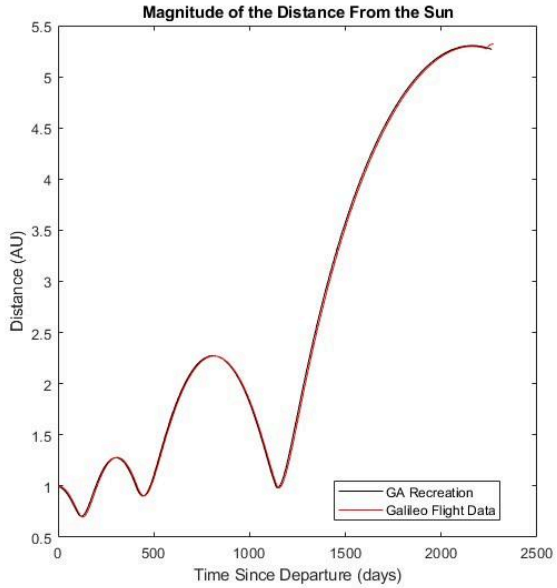

Fig. 3. Comparison of Position Magnitudes for the GA vs Galileo trajectories

Moving onto Fig. 4, it can be seen that differences between the two orbits never exceed ± 0.06 AU, or ± 8.98×10^6 km. For an interplanetary trajectory that orbits between 0.7 AU and 5.3 AU, the GA reconstruction of Galileo's trajectory never exceeds an error difference of ± 5%, as seen in Fig. 5. The results of this graph were produced by dividing the position magnitude differences in Fig. 4 by the position magnitudes of the Galileo trajectory.

After looking over the collected data, it can be concluded that the GA approach to solving for optimized interplanetary trajectories can produce good-quality data. Using NASA's Galileo as a baseline model to verify and validate the methods used in this paper, the GA employed was able to generate comparable data with high levels of accuracy. Although the methods used in this paper do not account for secondary targets or the gravitational perturbations of the other planets, as there was in the Galileo mission profile, the final results of the GA can be used as a preliminary solution for further, high-fidelity analysis.

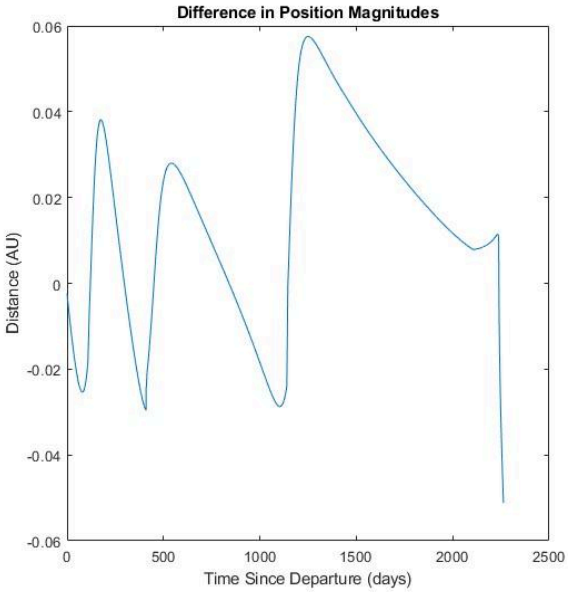

Fig. 4. Difference in the Position Magnitudes for the GA vs Galileo trajectories

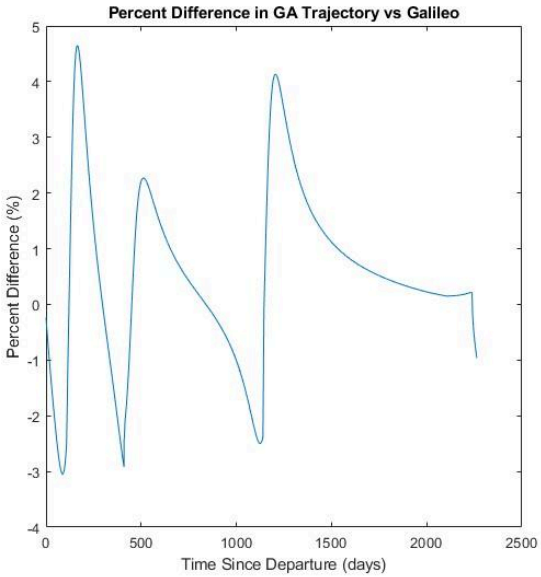

Fig. 5. Percent Difference between GA vs Galileo Trajectories

4. Project Results

With the GA method employed in this paper now verified and validated, the final step of the project is to collect the interplanetary trajectory information for a mission from Earth to Uranus. To get a range of possible solutions, the GA was run until 60 unique solutions were identified. To prevent the GA from finding duplicate trajectories, a list of the previously identified trajectories was saved and passed to the GA for review. If a chromosome repeated a known trajectory, and its total cost was less than what was saved, then the GA would take the solution and try to improve it. On the other hand, if a duplicate trajectory was identified and it had a cost score greater than what was saved, then it was assigned a large cost to prevent the GA from converging onto an already known trajectory. In addition to the constraint that limits the GA's ability to find repeated trajectories, the upper and lower bounds to each of the decision variables can be found in Table 4.1.

In addition to the GA constraints, the first of three assumptions made was about where the spacecraft started. For this project, it was assumed that the spacecraft began its trajectory from a circular parking orbit about Earth at an altitude of 250 km. The second assumption was that the spacecraft would be using an IUS, like the one that was used in Galileo's mission to Jupiter, to reduce the ΔV requirement of the spacecraft. The capability of the IUS is also assumed to have been improved slightly, giving a maximum orbital injection energy of 18 km^2/sec^2. The final assumption that was made about the spacecraft was its target orbit upon capture at Uranus. For this project, the spacecraft is planned to enter a highly elliptical orbit after its Uranus orbit insertion. The orbit will have a periapsis of 300,000 km and an eccentricity of 0.998. With these two parameters, the spacecraft's ΔV requirement to be captured about Uranus can be calculated.

Table 4.1 - Decision Variable Constraints for the Genetic Algorithm

	T_0	N	P_i	T_i	T_f
Lower Bound	Jan 1, 2030	2	Mercury	50	100
Upper Bound	Dec 31, 2034	10	Jupiter	2000	6000

The GA will be bound to find possible solutions in a 5-year launch window starting January 1st, 2030. During this window the GA will allow anywhere from 2 to 10 gravity assists, taking place at any planet between Mercury and Jupiter. The reason Saturn is not being considered for gravity assists is because it is out of position for an ideal transfer. During testing, gravity assists with Saturn would throw the spacecraft towards the orbits of Earth and Venus before it arrives at Uranus. These types of trajectories were not realistic and thus not considered for the analysis in this project. Then for each of the intermediate legs of the gravity assist, they were allowed to range from 50 to 2000 days, while the terminal leg of the trajectory was allowed to range from 100 days to 6000 days.

After running the program for 12 hours, 60 unique solutions were identified by the GA. The 10 trajectories with the lowest total ΔV requirements are found in Table 4.2. For reference, each planet visited during the trajectory is listed using its first letter, such as "E" for Earth and "J" for Jupiter. The following pages will contain a detailed view of the trajectories with the best and second best ΔV requirements. Appendix A will contain a detailed overview of the remaining 8 trajectories listed in Table 4.2. The first route, an Earth-Venus-Earth-Jupiter-Uranus trajectory, requires a time of flight of about 21 years and 2.5 km/sec of ΔV. The second best route is an Earth-Mars-Jupiter-Uranus trajectory, it requires about 22 years of travel time and has a ΔV requirement of about 3 km/sec.

Table 4.2. - Top 10 GA Results for Interplanetary Trajectories to Uranus

Route	Required ΔV (km/s)	Departure Date	Arrival Date	Time of Flight (years)
E-V-E-J-U	2.525	Apr 28, 2031	Jan 14, 2052	20.71
E-M-J-U	2.993	Jul 28, 2030	Apr 24, 2052	21.74
E-E-M-J-U	3.121	Apr 27, 2034	Aug 25, 2061	27.33
E-E-E-E-J-U	3.261	Oct 26, 2032	Jan 4, 2066	33.19
E-E-J-U	3.374	Aug 13, 2031	Mar 7, 2050	18.57
E-E-E-J-U	3.407	May 19, 2034	Jun 11, 2062	28.06
E-V-E-U	4.018	Jun 9, 2031	Jan 18, 2046	14.61
E-J-E-E-J-U	4.059	Jul 12, 2034	Dec 18, 2065	31.43
E-V-J-U	4.229	Nov 12, 2032	Dec 02, 2049	17.05
E-M-J-E-U	4.414	Dec 13, 2034	Dec 15, 2055	21.01

Table 4.3 - GA Result (E-V-E-J-U)

	Date	C3 (km^2/sec^2)	ΔV (km/sec)	Altitude (km)
Earth departure	Apr 28, 2031	17.4		250
Venus Close Approach	Sep 8, 2031	-	$5.4x10^{-6}$	4,624
Earth Close Approach	Apr 25, 2032	-	0.845	318.6
Jupiter Close Approach	Mar 4, 2036	-	1.010	2,334,495
Uranus Arrival	Jan 14, 2052	-	0.668	300,000

Upon reviewing the collected data, there were two interesting takeaways. The first was that in the top 13 trajectories with minimized ΔVs, 3 trajectories flew into one of their gravity assist planets. Although the penalty equation, Eq. (24), was used to offset the low ΔV cost, the penalty was small enough to make it appear comparable to the other trajectories found.

These three trajectories were omitted from Table 4.2 as they were not options to be considered. The second takeaway was from further analysis into the E-V-E-J-U and E-M-J-U trajectories and where they are required to use the most ΔV. In the E-V-E-J-U route, as seen in Table 4.3, the greatest ΔV expense is the maneuvers to send the spacecraft onto the subsequent legs of the trajectory after the Earth and Jupiter flybys. During these flybys, the ΔV requirement is 0.845 km/sec and 1.01 km/sec, respectively. The second-best route, E-M-J-U,

Table 4.4 - GA Result (E-M-J-U)

	Date	C3 (km^2/sec^2)	ΔV (km/sec)	Altitude (km)
Earth departure	Jul 28, 2030	73.33	2.155	250
Mars Close Approach	Jan 26, 2035	-	$4.9x10^{-5}$	327.75
Jupiter Close Approach	Jan 15, 2037	-	$1.1x10^{-5}$	4,340,986
Uranus Arrival	Apr 24, 2052	-	0.838	300,000

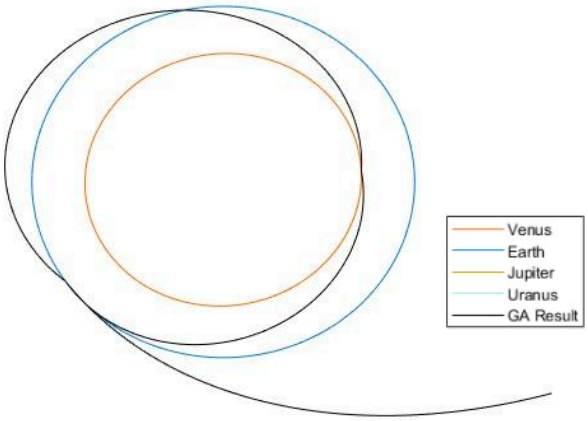

Fig. 6. Zoomed-in View of the E-V-E-J-U Trajectory

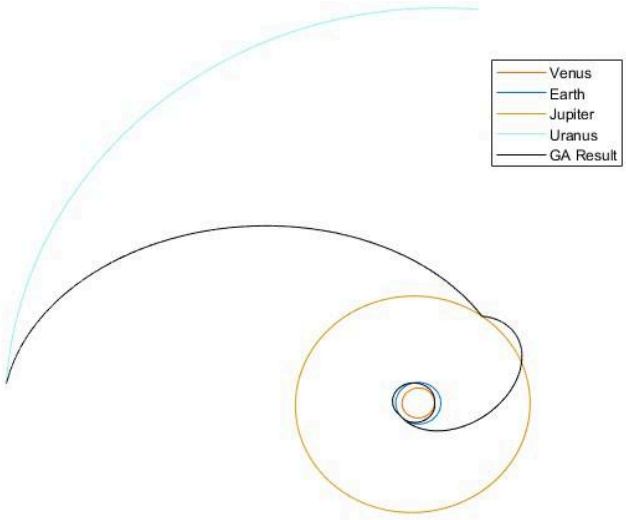

Fig. 7. Solar System View of the E-V-E-J-U Trajectory

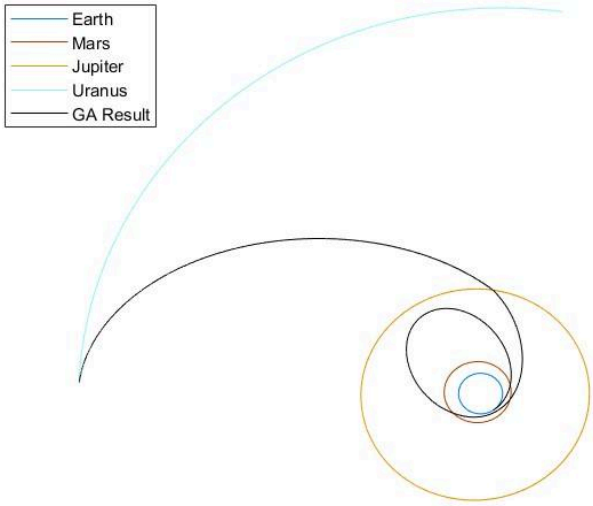

Fig. 8. Solar System View of the E-M-J-U Trajectory

has its greatest ΔV requirement departing from Earth. The provided injection energy by the IUS is not enough and the spacecraft would need to fill in the energy gap. The ΔV required during its 2 gravity assists are effectively 0, requiring only tens of mm/sec in ΔV. If the provided injection energy was any greater, this route and several others would have much lower total ΔV requirements, making them a more desirable trajectory option.

However, when performing gravity assists with Venus or Mercury, one additional factor to consider is the increased temperature. This factor alone can significantly complicate the design of the mission and, depending on the funding available, make gravity assists from

those planets not viable to meet the spacecraft's mission criteria.

5. Conclusion

While there are thousands of combinations of gravity assists that could get a spacecraft from Earth to Uranus, the GA employed for this project was able to identify 60 unique, preliminary trajectories. Each of the found trajectories had anywhere from 2 to 7 gravity assists, flying past Mercury and out to Jupiter to minimize the ΔV required by the spacecraft, and used the solutions to Lambert's problem to reach Uranus. However, while the solutions to Lambert's problem are ideal when operating with two-body dynamics, the real solar system applies gravitational perturbations throughout the interplanetary trajectory and constantly changes the shape of the orbit. In particular, spacecraft that fly in the outer solar system near Jupiter and Saturn can have their orbits greatly altered and thus likely require a deep space maneuver to stay on track to their target. The use of a deep space maneuver may also lower the overall ΔV requirement of the spacecraft. Allowing the spacecraft to make maneuvers outside of the flyby periapsis gives more opportunities for the spacecraft to perform smaller maneuvers and achieve the same goal as the multiple gravity assist approach followed in this project.

Although a deep space maneuver was explicitly stated to not be incorporated into the processes for this project, the two-body dynamics model was used so a deep space maneuver was not necessary for the interplanetary solutions. These results are neither perfect nor the global minimum solution, they are intended to serve as a starting point for further research and high-fidelity modeling.

One of the most interesting takeaways while analyzing the results of the GA was how much of an effect the injection energy has on the ΔV requirement of the spacecraft departing from its parking orbit around Earth. Looking back to the E-V-E-J-U and the E-M-J-U trajectories, while they have similar times of flight and required total ΔV, the ΔV distribution among the departure and gravity assists are completely different. The E-V-E-J-U trajectory did not require the maximum potential injection energy from IUS but required 2 large impulses during its approaches at Earth and Jupiter. The E-M-J-U trajectory, on the other hand, required an incredible amount of injection energy to start its trajectory but had near 0 km/sec ΔV requirements during its gravity assists. If the assumed injection energy of the IUS was any greater, the entries in Table 4.2 would need to be reorganized into a new list.

6. Future Work

Any further development on this project should first consider implementing deep space maneuvers as a part of the interplanetary trajectory. In addition to the multiple gravity assist approach performed for this project, incorporating deep space maneuvers gives a greater baseline on the possible trajectories to Uranus. After the incorporation of deep space maneuvers, the next step in further research should be to include a tuning algorithm to create smooth, continuous trajectories that account for spheres of influence, improve the process to solve Lambert's problem such that it can account for gravitational perturbations from across the solar system, and or develop an optimization algorithm that can optimize two different variables such as total time of flight and total ΔV required by the spacecraft at the same time.

Additionally, more work can be done to identify the numerous other ways of getting to Uranus. The results of this project were limited to determining only 60 possible trajectories because of the computationally intense nature of the GA employed.

7. Lessons Learned

During testing, it was discovered that the GA would converge to a different solution each time it ran. For the complex, non-linear process that is orbital mechanics, there are many solutions with local minimums that depend

on the starting parameters. Each time a population was generated, the randomized parameters could converge to a different answer. The multiple iterations to refine the time between the legs of an interplanetary trajectory, as outlined in Section 2, was the approach to try and counteract the random nature of the initial problem space and find the minimized solution for each identified route.

Additionally, after trial runs of the GA, a pattern was discovered in the collected data for optimized trajectories. Until the majority of the permutations were exhausted, the GA would tend to prioritize optimizing trajectories that used the minimum amount of possible gravity assists. This was likely due to the GA generating unrealistic trajectories that would have taken 200 days to go halfway across the solar system or require an impulse of 10 or more km/sec. The trajectories with the minimum number of gravity assists tend to produce a lower amount of required ΔV faster, as there are fewer opportunities for unrealistic maneuvers to disrupt the trajectory optimization process

Appendix A - Detailed List of Project Results

The following tables and figures provide a detailed look into the trajectories, from third-lowest through tenth-lowest, that required the least amount of ΔV out of the 60 identified as a part of the results found in Section 4.

Table A.1 - GA Result (E-E-M-J-U)

	Date	C3 (km^2/sec^2)	ΔV (km/sec)	Altitude (km)
Earth departure	Apr 27, 2034	74.2	2.185	250
Earth Close Approach	Mar 05, 2037	-	$4.7x10^{-5}$	3,720
Mars Close Approach	Sep 22, 2041	-	$1.2x10^{-7}$	1,420
Jupiter Close Approach	Jan 11, 2046	-	0.048	3,638,294
Uranus Arrival	Aug 25, 2061	-	0.888	300,000

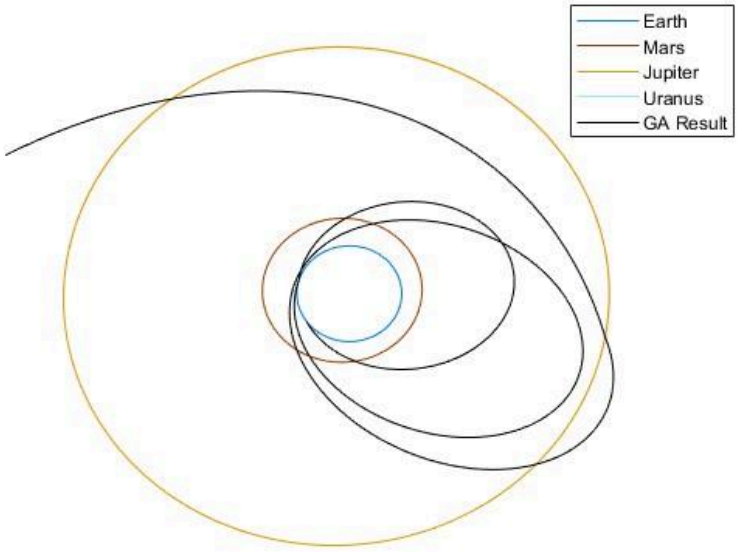

Fig. 9. Zoomed-in View of the E-E-M-J-U Trajectory

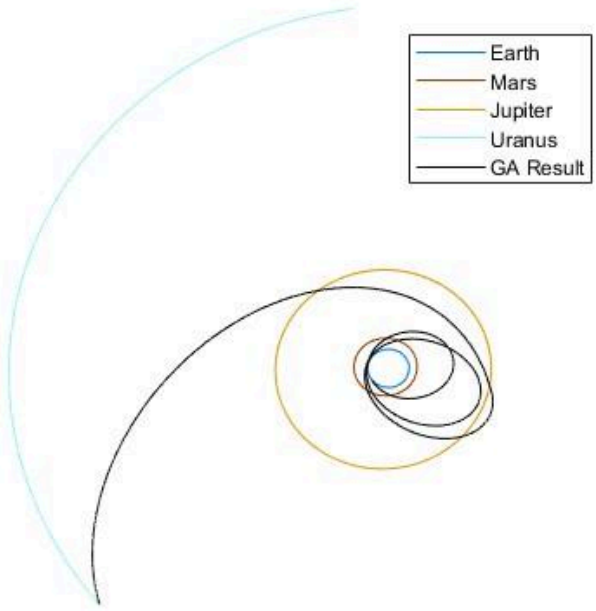

Fig. 10. Solar System View of the E-E-M-J-U Trajectory

Table A.2 - GA Result (E-E-E-E-J-U)

	Date	C3 (km^2/sec^2)	ΔV (km/sec)	Altitude (km)
Earth departure	Oct 26, 2032	86.92	2.635	250
Earth (1) Close Approach	Sep 23, 2037	-	0.018	1,741
Earth (2) Close Approach	Aug 21, 2042	-	0.005	1,583
Earth (3) Close Approach	Jul 19, 2047	-	$8.8x10^{-6}$	19,227
Jupiter Close Approach	Mar 28, 2050	-	$1.2x10^{-6}$	4,075,960
Uranus Arrival	Jan 04, 2066	-	0.603	300,000

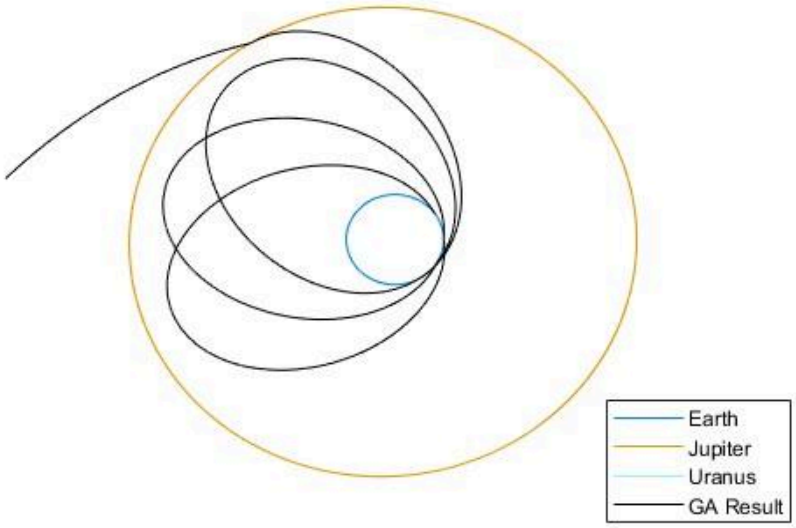

Fig. 11. Zoomed-in View of the E-E-E-E-J-U Trajectory

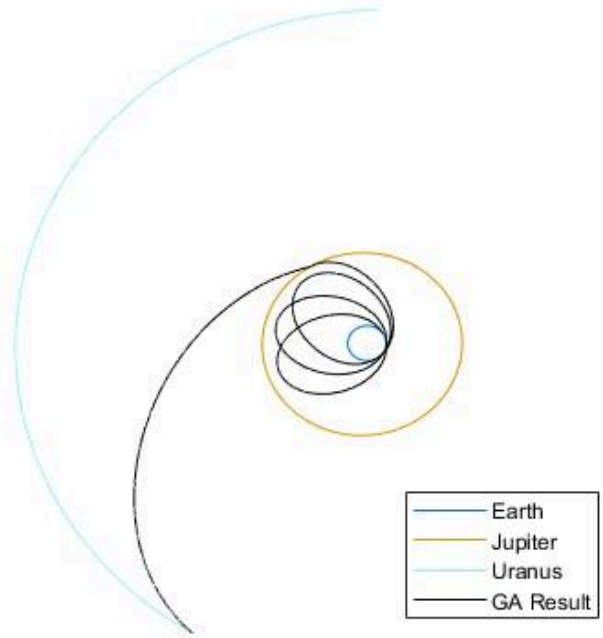

Fig. 12. Solar System View of the E-E-E-E-J-U Trajectory

Table A.3 - GA Result (E-E-J-U)

	Date	C3 (km^2/sec^2)	ΔV (km/sec)	Altitude (km)
Earth departure	Aug 13, 2031	83.59	2.519	250
Earth Close Approach	Jun 13, 2034	-	0.002	2,952
Jupiter Close Approach	Jun 08, 2036	-	$2.9x10^{-7}$	3,760,147
Uranus Arrival	Mar 07, 2050	-	0.853	300,000

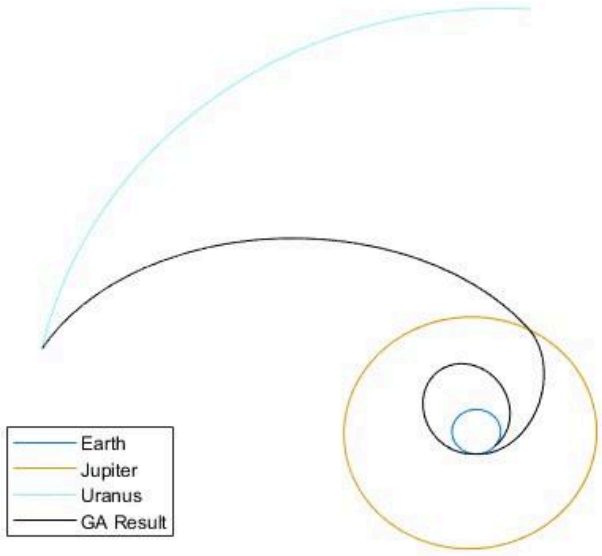

Fig. 13. Solar system View of the E-E-J-U Trajectory

Table A.4 - GA Result (E-E-E-J-U)

	Date	C3 (km^2/sec^2)	ΔV (km/sec)	Altitude (km)
Earth departure	May 19, 2034	82.39	2.477	250
Earth (1) Close Approach	Mar 20, 2037	-	0.126	328
Earth (2) Close Approach	Feb 18, 2042	-	$9.2x10^{-7}$	14,638
Jupiter Close Approach	Jan 06, 2046	-	$6.3x10^{-6}$	3,530,981
Uranus Arrival	Jun 11, 2062	-	0.804	300,000

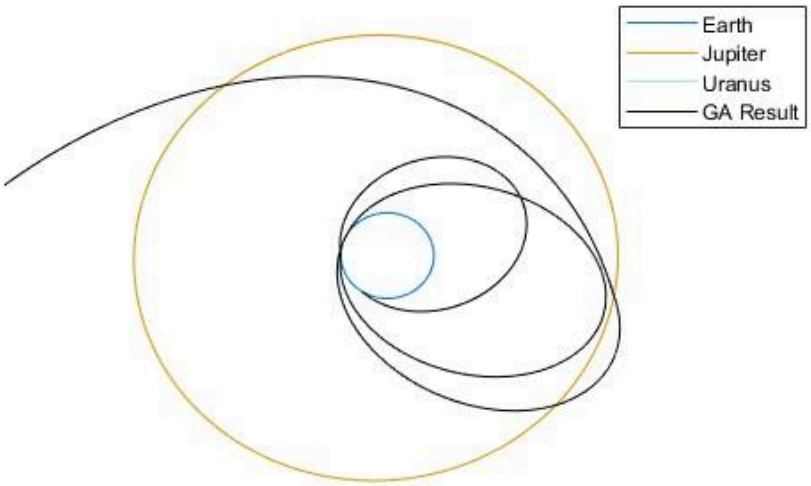

Fig. 14. Zoomed-in View of the E-E-E-J-U Trajectory

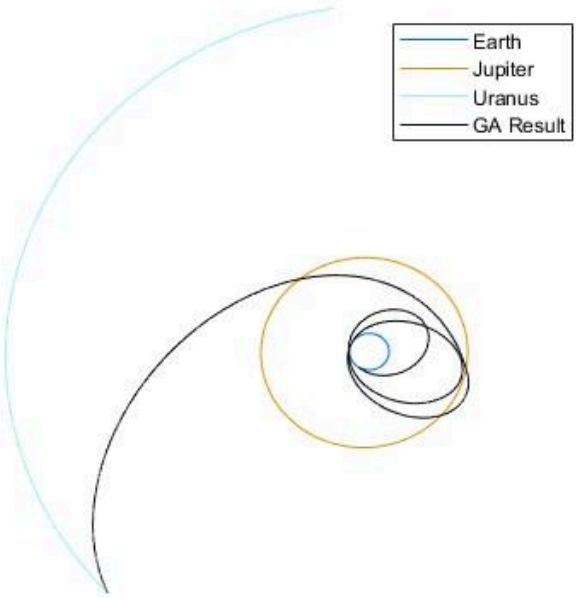

Fig. 15. Solar System View of the E-E-E-J-U Trajectory

Table A.5 - GA Result (E-V-E-U)

	Date	C3 (km^2/sec^2)	ΔV (km/sec)	Altitude (km)
Earth departure	Jun 09, 2031	22.55	0.192	250
Venus Close Approach	Aug 26, 2031	-	1.621	331
Earth Close Approach	Jul 08, 2034	-	0.096	319
Uranus Arrival	Jan 18, 2046	-	2.109	300,000

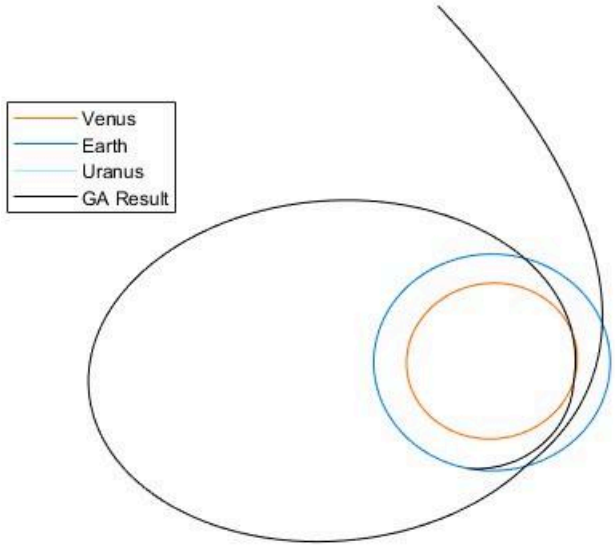

Fig. 16. Zoomed-in View of the E-V-E-U Trajectory

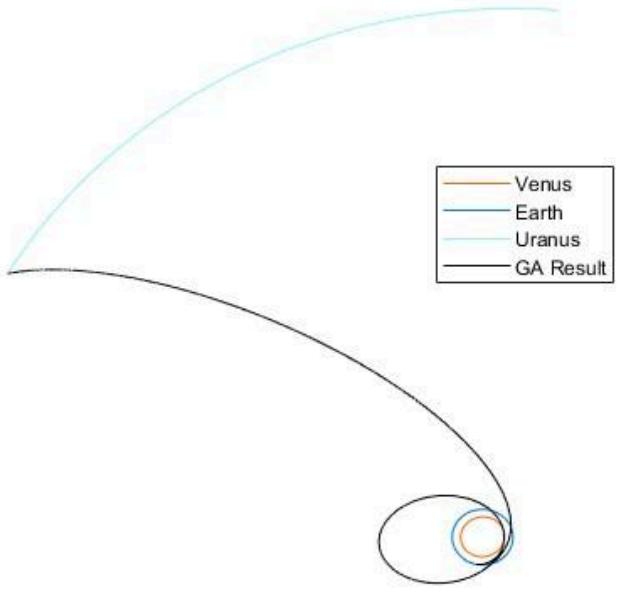

Fig. 17. Solar System View of the E-V-E-U Trajectory

Table A.6 - GA Result (E-J-E-E-J-U)

	Date	C3 (km^2/sec^2)	ΔV (km/sec)	Altitude (km)
Earth departure	Jul 12, 2034	85.30	2.579	250
Jupiter (1) Close Approach	Jun 03, 2038	-	0.659	2,941,298
Earth (1) Close Approach	Sep 10, 2043	-	$1.1x10^{-4}$	17,129
Earth (2) Close Approach	Jul 04, 2047	-	$8.8x10^{-6}$	28,693
Jupiter (2) Close Approach	Jun 01, 2050	-	0.192	3,853,784
Uranus Arrival	Dec 18, 2065	-	0.628	300,000

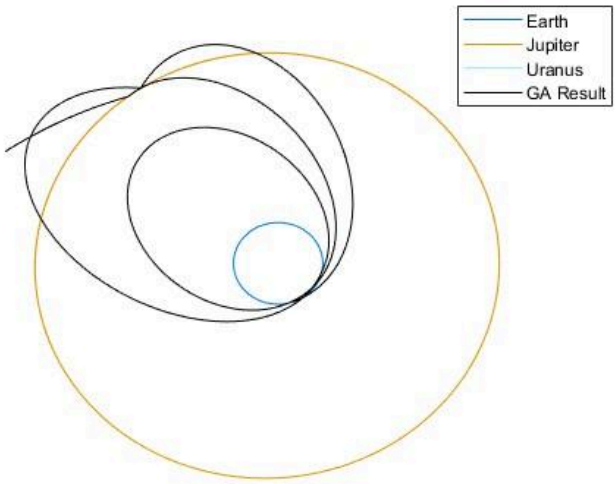

Fig. 18. Zoomed-in View of the E-J-E-E-J-U Trajectory

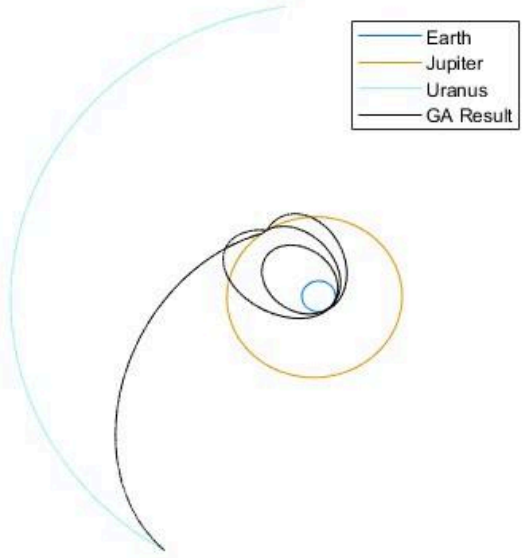

Fig. 19. Solar System View of the E-J-E-E-J-U Trajectory

Table A.7 - GA Result (E-V-J-U)

	Date	C3 (km^2/sec^2)	ΔV (km/sec)	Altitude (km)
Earth departure	Nov 12, 2032	31.09	0.544	250
Venus Close Approach	Apr 25, 2033	-	2.463	302.68
Jupiter Close Approach	Aug 12, 2036	-	0.303	1,977,486
Uranus Arrival	Dec 02, 2049	-	0.919	300,000

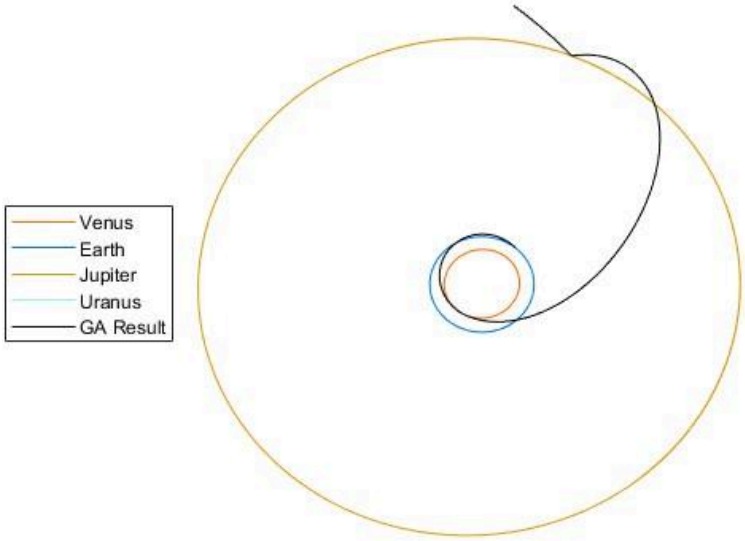

Fig. 20. Zoomed-in View of E-V-J-U Trajectory

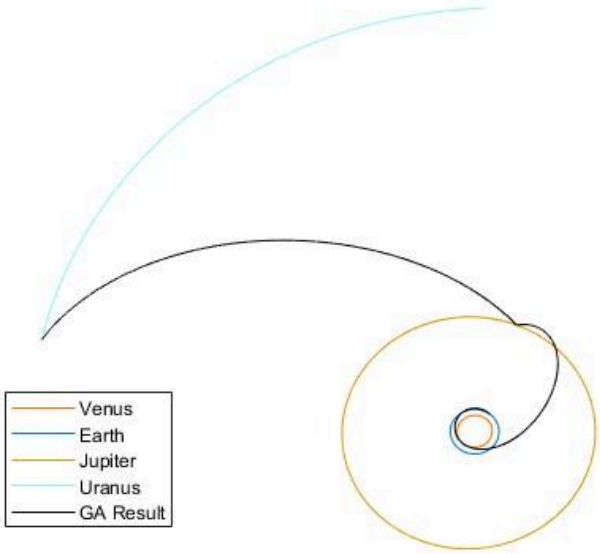

Fig. 21. Solar System View of E-V-J-U Trajectory

Table A.8 - GA Result (E-M-J-E-U)

	Date	C3 (km^2/sec^2)	ΔV (km/sec)	Altitude (km)
Earth departure	Dec 13, 2034	64.83	1.846	250
Mars Close Approach	Aug 20, 2035	-	0.491	170
Jupiter Close Approach	Mar 16, 2040	-	0.202	5,111,399
Earth Close Approach	Nov 07, 2043	-	$1.3x10^{-5}$	7,276
Uranus Arrival	Dec 15, 2055	-	1.875	300,000

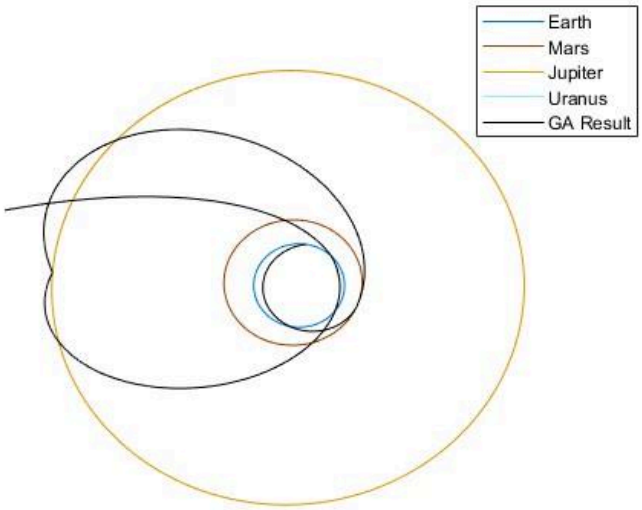

Fig. 22. Zoomed-in View of the E-M-J-E-U Trajectory

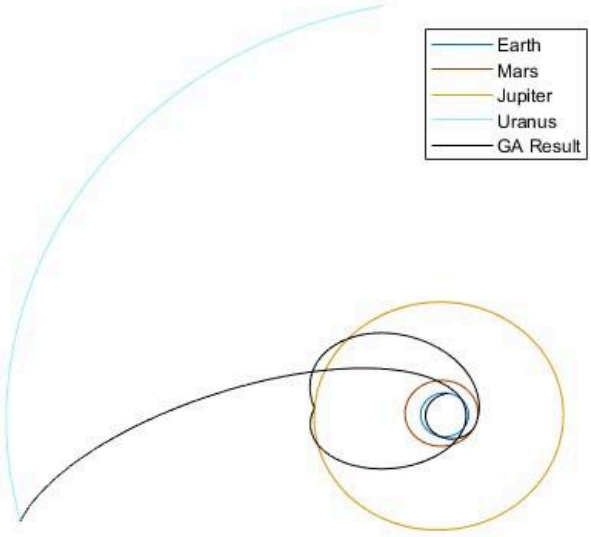

Fig. 22. Solar System View of E-M-J-E-U Trajectory

References

[1] National Aeronautics and Space Administration. *Uranus Facts* [Online]. Available: https://science.nasa.gov/uranus/facts/#hds-sidebar-nav-5

[2] National Aeronautics and Space Administration. *Voyager 2* [Online]. Available: https://science.nasa.gov/mission/voyager/voyager-2/

[3] Jet Propulsion Laboratories. *Mission to Jupiter, Juno* [Online]. Available: https://www.jpl.nasa.gov/missions/juno

[4] European Space Agency. *JUICE. Jupiter Icy Moons Explorer* [Online]. Available: https://www.esa.int/Science_Exploration/Space_Science/Juice

[5] National Aeronautics and Space Administration. *Europa. Moon of Jupiter. Potential for life* [Online]. Available: https://europa.nasa.gov/

[6] National Academies of Sciences, Engineering, and Medicine. 2023. *Origins, Worlds, and Life: A Decadal Strategy for Planetary Science and Astrobiology 2023-2032* [Online]. Washington, DC: The National Academies Press. Available: https://doi.org/10.17226/26522

[7] A. Simon, F. Nimmo, and R. C. Anderson. *Journey to An Ice Giant System. Uranus Orbiter & Probe* [Online]. June 7, 2021. Available: https://drive.google.com/file/d/1TxDt_qU6H2j2fYGqcDUTJQioSJ2W_KnN/view?usp=drive_link

[8] National Aeronautics and Space Administration. *Basics of Spaceflight: A Gravity Assist Primer* [Online]. Available: https://science.nasa.gov/learn/basics-of-space-flight/primer/

[9] Goldberg, D., *Genetic Algorithms in Search, Optimization, and Machine Learning*, 1st ed., Addison Wesley, Reading, MA, 1989, pp. 59–88

[10] Koza, J., *Genetic Programming: On the Programming of Computers by Means of Natural Selection*, 1st ed., MIT Press, Cambridge, MA, 1992, pp. 80–119

[11] Syswerda, G., “Uniform Crossover in Genetic Algorithms,” Proceedings of the 3rd International Conference on Genetic Algorithms, Morgan Kaufmann, San Francisco, 1989, pp. 2–9

[12] J. E. Prussing and B. A. Conway, Orbital mechanics, Second edition. New York: Oxford University Press, 2013.

[13] R. H. Gooding, “A procedure for the solution of Lambert’s orbital boundary-value problem,” Celestial mechanics and dynamical astronomy, vol. 48, no. 2, pp. 145–165, 1990, doi: 10.1007/BF00049511.

[14] The Navigation and Ancillary Information Facility, “SPICE. An Observation Geometry System for Space Science Missions" [Online]. Available: https://naif.jpl.nasa.gov/naif/

[15] C.H. Acton, "Ancillary Data Services of NASA's Navigation and Ancillary Information Facility;" Planetary and Space Science, Vol. 44, No. 1, pp. 65-70, 1996. DOI 10.1016/0032-0633(95)00107-7

[16] C. Acton, N. Bachman, B. Semenov, and E. Wright; A look toward the future in the handling of space science mission geometry; Planetary and Space Science (2017); DOI 10.1016/j.pss.2017.02.013

[17] R.S. Park, W.M. Folkner, J.G. Williams, and D.H. Boggs, The JPL Planetary and Lunar Ephemerides DE440 and DE441, Astronomical Journal. DOI: 10.3847/1538-3881/abd414

[18] R.S. Park, and W.M. Folkner, Planetary ephemeris DE440 for Mars2020, JPL Interoffice Memorandum, 392R-20-002, July 2020.

[19] Moyer, T.D., *Transformation from Proper Time on Earth to Coordinate Time in Solar System Barycentric Space-Time Frame of Reference*, Parts 1 and 2, Celestial Mechanics 23 (1981), 33-56 and 57-68.

[20] Moyer, T.D., *Effects of Conversion to the J2000 Astronomical Reference System on Algorithms for Computing Time Differences and Clock Rates*, JPL IOM 314.5--942, 1 October 1985.

[21] S. Wagner, B. Kaplinger, and B. Wie, “GPU Accelerated Genetic Algorithm for Multiple Gravity-Assist and Impulsive V Maneuvers,” 2012.

[22] S. Wagner and B. Wie, “Hybrid algorithm for multiple gravity-assist and impulsive Delta-V maneuvers,” Journal of guidance, control, and dynamics, vol. 38, no. 11, pp. 2096–2107, 2015, doi: 10.2514/1.G000874.

[23] The MathWorks, Inc. “Genetic Algorithm” [Online]. Available: https://www.mathworks.com/discovery/genetic-algorithm.html

[24] Gad, A., and Abdelkhalik, O., “Hidden Genes Genetic Algorithm for Multi-Gravity-Assist Trajectories Optimization,” *Journal of Spacecraft and Rockets*, Vol. 48, No. 4, July–Aug. 2011, pp. 629–641. doi:10.2514/1.52642

[25] The MathWorks, Inc. “fsolve” [Online]. Available: https://www.mathworks.com/help/optim/ug/fsolve.html

[26] Englander, J., Conway, B., and Williams, T., “Optimal Autonomous Mission Planning via Evolutionary Algorithms,” *21th AAS/AIAA SpaceFlight Mechanics Meeting*, American Astronomical Soc. Paper 2011-159, Washington, D.C., Feb. 2011.

[27] D. Eagle, Gravity-assist Trajectory Design and Analysis - SNOPT [Online]. MATLAB Central File Exchange, 2023. Available: https://www.mathworks.com/matlabcentral/fileexchange/39462-gravity-assist-trajectory-design-and-analysis-snopt?status=SUCCESS

[28] L. A. D’Amario, L. E. Bright, and A. A. Wolf, “Galileo trajectory design: The Galileo mission,” Space science reviews, vol. 60, no. 1–4, pp. 23–78, 1992.

[29] M. Meltzer, Mission to Jupiter : A History of the Galileo Project. Washington, DC: National Aeronautics and Space Administration, NASA History Division, 2007.

[30] J. Pojman, Galileo Interplanetary cruise SPK file. Jet Propulsion Laboratory, 2000

[31] J. Pojman and J. Johannesen, Galileo Primary Tour SPK file. Jet Propulsion Laboratory, 2000